

## **CLIMATE DYNAMICS OF SOUTHERN REGION OF MOZAMBIQUE: SPECTRAL AND FRACTAL ANALYSIS**

MEDJA, Jone Lucas<sup>1</sup> e BASSREI, Amin<sup>2</sup>

<sup>1</sup> Universidade Eduardo Mondlane, Moçambique / Faculdade de Agronomia e Engenharia Florestal.  
Email: [jonemedja@gmail.com](mailto:jonemedja@gmail.com)

<sup>2</sup> Universidade Federal da Bahia, Brasil / Instituto de Geociências. Email: [bassrei@ufba.br](mailto:bassrei@ufba.br)

**ABSTRACT:** In this study, we have applied the spectral and fractal analyses to time series of precipitation and extreme temperatures in order to understand the climate behavior of the southern region of Mozambique in the face of the climate change at global level. Observations along the period of 1960 - 2018 were used. We have determined the periodicity, the long term variability and the persistence of the climate variables. The rainy season behavior was also assessed. The results are related to the current global climate observations and projections contained in the fifth assessment report of the Intergovernmental Panel on Climate Change (IPCC-AR5). In particular, the signal of climate change in Mozambique is visible. Precipitation did not show a significant trend in its variability. However, a slight decrease is noticeable in the provinces of Gaza and Inhambane. The rainy season showed a tendency to a late start and an early end, resulting in a decrease of the season length. Extreme temperatures, on the other hand, showed a clear upward trend, with the increase being more pronounced for the minimum temperature than the maximum temperature. The maximum temperature increased by about 0.65 °C and the minimum temperature increased by about 1.2 °C during the analyzed period. All variables showed persistency indicating that the observed behavior is likely to continue for a long period in future.

**Keywords:** climate dynamics, spectral analysis, fractal analysis, southern region of Mozambique.

## INTRODUCTION

Many extreme climate events currently occurring have been linked to a possible global climate change, and this topic has been of much debate worldwide. According to the fifth assessment report of the Intergovernmental Panel on Climate Change (IPCC-AR5), the evidences of climate change has grown significantly in recent years in observations made in the atmosphere and on the surface (Hartmann et al., 2013). The implications of climate change are evident in the socio-economic, environmental, health, agriculture, and among others areas. In particular for Mozambique, several extreme events (such as the cyclone Eline in 2000, the cyclone Fávio in 2007, the floods in the northern region of the country in 2014, drought in the southern and central regions in 2015, and the recent cyclones Idai and Keneth in 2019) had caused catastrophic consequences, with huge economic losses including death of hundreds of people.

Among the climate observations, the air temperature and precipitation regimes are the most important. According to Hartmann et al. (2013), the global mean surface air temperature over land and oceans shows from a linear trend, an increase of about 0.85 °C, during the period from 1880 to 2012. The diurnal temperature range has been decreasing since 1950, with a rapid increase in minimum temperature compared to the increase in maximum temperature. On the contrary to the global mean surface air temperature that shows an upward trend on its variability, the global average of precipitation does not present a clear trend, it shows an increase in some regions and a decrease in others. In particular, during the period from 1901 to 2005 a decreasing rainfall tendency was observed in the Sahel region of Africa (Christy et al., 2009).

In some cases, the climate scenario observed in some specific regions does not agree with the global climate trends. In other words, for certain regions, the climate variables may show singular trends, which are different from the global behavior. For example, air temperature is the most evidenced parameter in discussions about climate change, admitting the occurrence of global warming caused by the intensification of CO<sub>2</sub> concentration due to the industrial development and to the technological advancements (Smithson, 2002). However, for some specific regions, analyzes in certain periods show negative trends in the mean temperature. Precipitation also does not present a clear trend. It is less representative and varies a lot, both spatially and temporarily. This uncertainty is a concern for several sectors of activity, especially for a developing country. For instance, in Mozambique, the agricultural sector is the most sensitive to climate change. The majority of population practice agriculture conditioned by the climate regime, without any mechanization. The knowledge of climate variability in a particular region is crucial for decision making. In particular for agriculture, the knowledge of the regimes of precipitation and temperature is a determining factor to ensure better productivity.

Even with some advancement on climate studies in Mozambique, the knowledge of the evolution of these climate parameters in connection with the global climate change is still a gap. Given this climate diversity, it is important to carry out a deep analysis to understand the current scenario of climate dynamics in the three major regions of Mozambique (northern, central and southern). In this study, we evaluate the climate dynamics limited to the southern region of the country. The spectral and fractal analyses are applied to the time series of precipitation and extreme temperatures to determine the periodicity, the persistence and the long term variability. In addition, the rainy season behavior was also assessed, taking into account the following parameters: (i) the total precipitation of the rainy season; (ii) the duration of the rainy season; (iii) the average intensity of precipitation, and (iv) the occurrence of dry days within the rainy season (Indian summer). The obtained results are related to the global observations and projections contained in the fifth assessment report of the Intergovernmental Panel on Climate Change (IPCC-AR5), the latest report published in the moment of this research.

## **DATA AND METHODS**

### **Climate series**

The climate data used for this study consists of daily records of precipitation and extreme temperatures from fifteen meteorological stations distributed throughout the southern region of Mozambique. The southern region of Mozambique is located between the parallels 21° 05'S and 26° 52'S and the meridians 31° 20'E and 35° 20'E, on the southeastern coast of Africa. Figure 1 shows the study area, it comprises the provinces of Maputo, Gaza and Inhambane, on the south of the Save River. The data was provided by the Instituto Nacional de Meteorologia (INAM) and corresponds to the period of 1960 - 2018. The meteorological stations are distributed in the three provinces, as follows: five stations in Maputo, six in Gaza and four in Inhambane. The Table 1 shows the list of stations and their respective geographical positions.

**Table 1:** List of meteorological stations and their respective geographical positions.

#	ID	Station Name	Latitude (°S)	Longitude (°E)	Elevation (m)
1	GZ-MANJ	Manjacaze	24.72	33.88	65
2	GZ-MACI	Macie	25.03	33.10	56
3	GZ-XAI	Xai-Xai	25.05	33.63	4
4	GZ-MANIQ	Maniquenique	24.73	33.53	13
5	GZ-CHOK	Chokwe	24.52	33.00	33
6	GZ-MASSG	Massingir	23.92	32.16	252
7	IB-INHAM	Inhambane	23.87	35.38	14
8	IB-INHAR	Inharrime	24.48	35.02	43
9	IB-PAND	Panda	24.05	34.72	150
10	IB-VILA	Vilânculos	22.00	35.32	20
11	MP-UMBE	Umbeluzi	26.05	32.38	12
12	MP-MANH	Manhiça	25.37	32.80	35
13	MP-OBS	Map/Observatório	25.97	32.70	47
14	MP-MAV	Map/Mavalane	25.92	32.57	39
15	MP-CHANG	Changalane	26.30	32.18	100

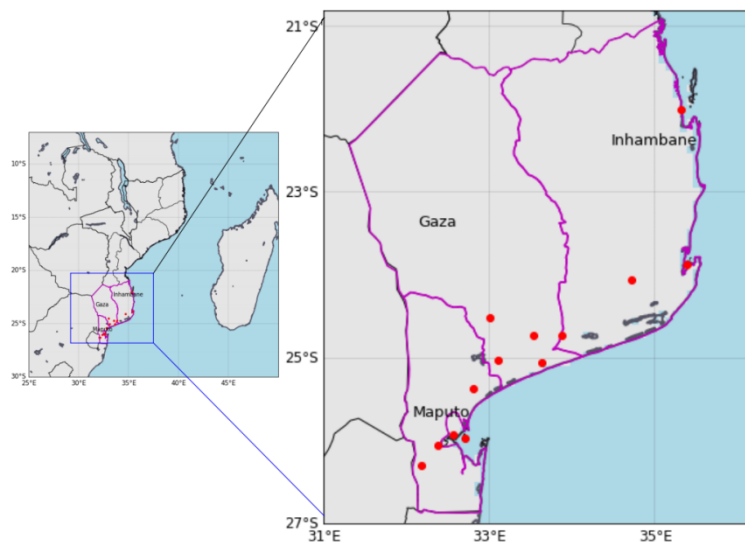


**Figure 1-** Map of the study area. The detail shows the southern region of Mozambique.

### Determination and characterization of the rainy season

The beginning and end dates of the rainy season were determined for each year and for each province in the study region. Several models are found in the literature to determine the beginning and end of the rainy season, such as the criteria used by Sansigolo (1989) and by Marengo et al. (2001).

In this work, we have adopted a new method for estimating the beginning and end dates of the rainy season. This new approach starts by considering at first the ombrothermic diagram proposed by Bagnouls and Gaussen (1957), where dry and wet periods are defined. This

criterion is based on the regimes of temperature and precipitation throughout the year, taking into account the favorable and unfavorable states for the development of natural vegetation. In the ombrothermic diagram the abscissa indicates the months of the year, and the ordinates (main and secondary axes) indicate the average monthly precipitation  $P$  in mm and the average monthly temperature  $T$  in °C respectively. The scale is arranged so that the temperature values correspond to half of the precipitation, for example, 20 °C in temperature axis corresponds to 40 mm in precipitation axis. From this arrangement, the months whose precipitation column is below the temperature curve, that is, if  $P < 2T$ , they are considered dry months. This relationship is also used by Köppen in his climate classification criterion for defining the limits of dry regions (inside the climate group B) where the potential evaporation exceeds the precipitation. On the other hand, if  $P \geq 2T$ , the months are considered wet. Based on this last relationship, a reference interval of wet months throughout the year was defined.

Thus, the beginning of the rainy season was considered to be the first day with a record of at least 1 mm of precipitation within the month whose total precipitation is equal to or greater than twice the average temperature of the same month ( $P \geq 2T$ ), counting from the starting month of the pre-established reference range of wet period. In this particular case the starting month was September. The end date was determined by the reverse procedure. The algorithm for executing this method was implemented in FORTRAN.

The duration of the rainy season in days was determined by the summation of all days from the beginning date up to the end date of the rainy season. The total precipitation during the rainy season in mm is calculated by the summation of the daily precipitation occurred during the rainy season. The average intensity of precipitation during the rainy season in mm/day was calculated by the ratio between the total precipitation and the duration of the rainy season.

For Indian summer, the occurrence of at least ten consecutive days without precipitation within the rainy season was considered. This was based on the fact that the water need of plants can, in periods of up to ten days be satisfied by the soil moisture (Machado et al., 1996).

### Spectral analysis

In the spectral analysis a signal is transformed from time domain to frequency domain. Considering that a given time series can be represented by a generic function  $x(t)$ , the relationship that allows this function to be transformed from the time domain to the frequency domain, denoted as  $X(f)$ , is called Fourier Transform (Bracewell, 1999):

$$X(f) = \int_{-\infty}^{+\infty} x(t) e^{-i2\pi ft} dt.$$

The meteorological or climate elements are, from the statistical point of view, continuous and random variables. However, since the climate observations are made at discrete time intervals, the result is a discrete time series, so that we will make use of the Discrete Fourier Transform (DFT). The DFT is applied in a discrete series, both periodic and non-periodic. The DFT of a discrete sequence  $x_k$  with  $N$  samples, denoted by  $X_n$ , is calculated by the following relationship:

$$X_n = \sum_{k=0}^{N-1} x_k e^{-i\frac{2\pi}{N}nk}, \quad 0 < n < N-1.$$

The computational implementation of the DFT was performed through the Fast Fourier Transform (FFT) in Python. In the frequency domain the signal is represented by the Fourier spectrum which relates the frequency and the amplitude of the signal. For each frequency  $f_n$ , its amplitude  $A_n$  is determined by the expression:

$$A_n = \sqrt{\text{Re}(X_n)^2 + \text{Im}(X_n)^2}, \quad 0 < n < N-1.$$

Here, the climate data is sampled monthly, so the frequency is given in cycle/month instead of the fundamental unit of cycle/second. Considering the period of 1960 – 2018, with the sampling interval of  $\Delta t = 1$  month, we have  $N = 696$  observations, and thus the  $n$ -th frequency in cycle/month will be:

$$f_n = \frac{n}{N\Delta t} = \frac{n}{696 \times 1} = 0.00144n, \quad 0 < n < N-1.$$

In the inverse Fourier transform, that is, in the transition from the frequency domain back to the time domain, the spectrum was filtered in order to attenuate the effect of high frequencies. The low frequency content allows determining the long term variability pattern of the series. In this particular case, frequencies ranging from 0.0 to 0.0083 cycles/month were selected in order to define a decadal variability.

## Fractal Analysis

The concept of fractal was introduced by Mandelbrot (1967). A fractal is an object whose geometry presents infinite self-similarities at different scales. The fractal analysis has been widely used by researchers from different areas to investigate the long memory of natural phenomena.

In this work the fractal analysis was derived from the rescaled ( $R/S$ ) analysis. The  $R/S$  analysis was formulated by Hurst (1951) while studying dams dimensioning over the Nile River. Hurst's initial idea was to determine the maximum and minimum volumes in reservoirs (ideal capacity) taking into account the annual flows associated with the River during a certain period of some decades. For this purpose, Hurst analyzed a statistical variable called “adjusted range” ( $R$ ) from the cumulative river flows over time. Then Hurst normalized this value of  $R$  by the standard deviation ( $S$ ) of the sequence to obtain what he called “Rescaled Adjusted Range”, which is the  $R/S$  statistics, a dimensionless quantity.

Considering a certain sequence  $X_t$  ( $t = 1, 2, 3, \dots, N$ ) of random numbers (with  $N$  observations), not necessarily independent, and defining the  $k$ -th partial sum as  $Y_k = X_1 + X_2 + \dots + X_k$  ( $k = 1, 2, 3, \dots, \tau$ ),  $\tau$  being the number of elements of the sequence. Then, we define  $R_\tau$  as:

$$R_\tau = \max_{1 \leq k \leq \tau} \left\{ Y_k - \frac{k}{\tau} Y_\tau \right\} - \min_{1 \leq k \leq \tau} \left\{ Y_k - \frac{k}{\tau} Y_\tau \right\},$$

and the  $R/S_{(\tau)}$  is given by:

$$R/S_{(\tau)} = \frac{R_{\tau}}{\sqrt{\frac{1}{\tau} \sum_{k=1}^{\tau} (X_k - \frac{1}{\tau} Y_{\tau})^2}}.$$

In analyzing this statistics for observations involving different natural phenomena, Hurst found that there was a function relating the values of  $R/S$  to the number of observations that entered in the calculations, and it is given by the following expression:

$$R/S_{(\tau)} = \left(\frac{\tau}{2}\right)^H,$$

where  $H$  is a constant known as Hurst exponent.

Mandelbrot and Wallis (1969) found that this empirical relationship discovered by Hurst was applicable to processes or phenomena characterized by Fractional Brownian Motion. Such functions exist if and only if  $0 < H < 1$ . In this case, the Hurst exponent has the following interpretation: (a) If  $0.5 < H < 1$  the series is said to be persistent, it indicates positive long-term correlations, what means that an increase in the past will tend to be followed by another increase in the future, the opposite situation is also true, a decrease in the past will tend to be followed by another decrease in the future; (b) If  $0 < H < 0.5$  the series is said to be anti-persistent, high and low values occur alternately in adjacent pairs, meaning that an increase in the past implies an average decrease in the future and vice-versa; (c) If  $H = 0.5$  the series has a purely random behavior (also known as white noise).

Additionally,  $H$  provides information about the fractal dimension of the series under analysis by the expression,  $D = 2 - H$  (Feder, 1989), where  $1 < D < 2$ . The fractal dimension indicates the level of complexity of the phenomenon and it gives us the idea about the existence of self-similarities in the sequence at an increasingly small scale.

## RESULTS AND DISCUSSIONS

### Seasonality

The southern region of Mozambique has clearly shown two distinct seasons, one relatively cold and dry and the other relatively hot and wet. Figure 2 shows the ombrothermic diagrams of the three provinces in the study region, and these diagrams show a relatively short winter and a long summer. The dry and relatively cold period extends from May to September, with the month of August being the driest and July the coldest of the year in the region. The rainy and relatively hot period extends from October to April, being the months of January and February the most humid and the warmest of the year. Based on the Köppen's criterion for climate classification, the pattern of precipitation and temperature shown in the diagrams results in a climate of type Aw for the southern region of Mozambique, which corresponds to the tropical humid climate with a dry season in the winter, having Savanna as the typical vegetation.



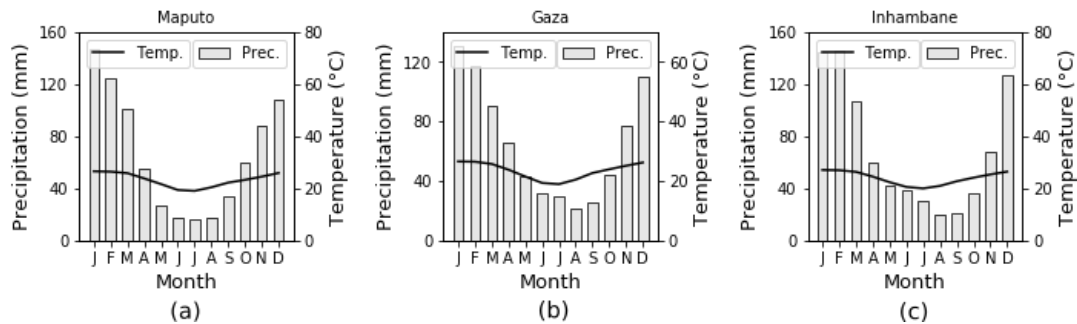


**Figure 2** - Ombrothermic diagrams of the three provinces in the southern region of Mozambique: (a) Maputo, (b) Gaza, (c) Inhambane. The bars represent the precipitation (mm) and the line represents the temperature (°C).

Using the proposed methodology to determine the beginning and end of the rainy season, we found the beginning date being on average into the first week of October and the end date being on average into the last week of April. Figure 3 shows the occurrence of dry, rainy and Indian summer periods in the southern Mozambique over the period of 1960 - 2018. The occurrence of sequences of at least 10 dry days (Indian summer) within the rainy season has been identified in some years and it presents an approximately uniform distribution throughout the evaluated period, with greater predominance in the province of Gaza.

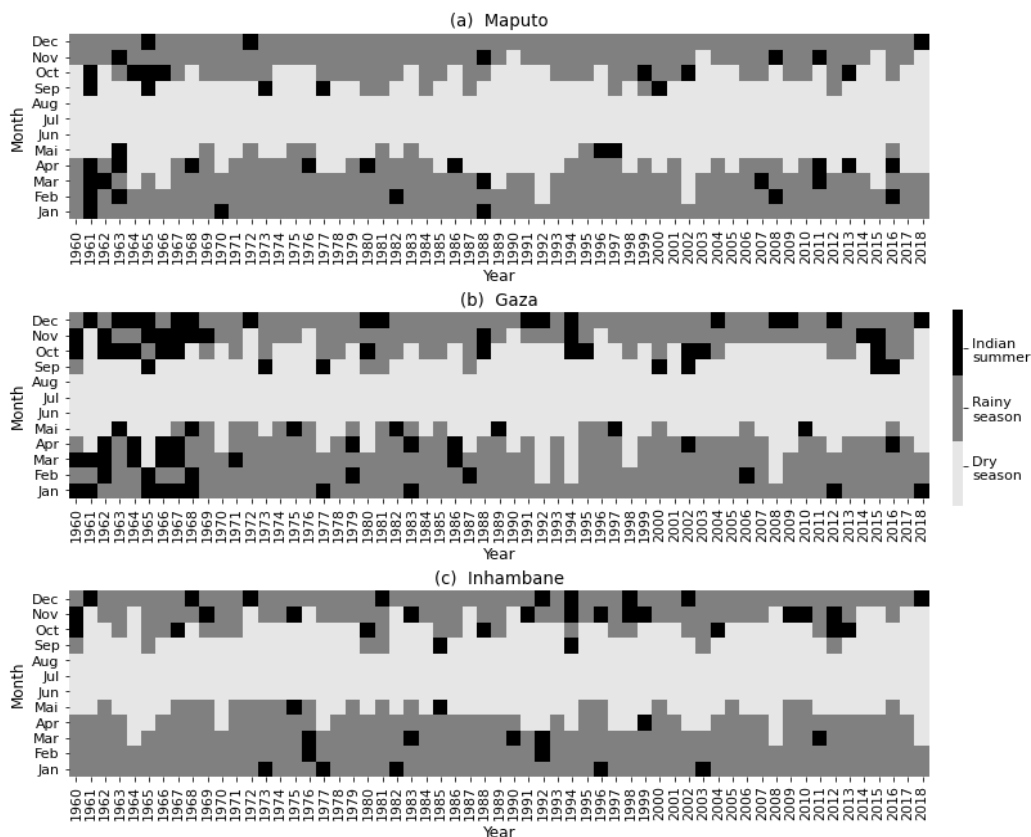


**Figure 3** - Occurrence of dry, rainy and Indian summer periods of the three provinces in the southern region of Mozambique: (a) Maputo, (b) Gaza and (c) Inhambane. The data is related to 1960-2018.



## Periodicity

The periodicity was determined from the Fourier spectrum. For both precipitation and temperatures, it was possible to identify the frequency of  $f = 0.083$  cycles per month as the most significant in all cases, and it corresponds to the periodicity  $T = 1/f$  of 12 months that is the annual variability, as expected. A small semiannual variability (six months) was also observed at the frequency of approximately  $f = 0.166$  cycles per month, being more pronounced for temperatures than for precipitation. Figure 4 shows the Fourier spectrum of precipitation and the maximum and minimum temperatures for the three provinces of the study region.

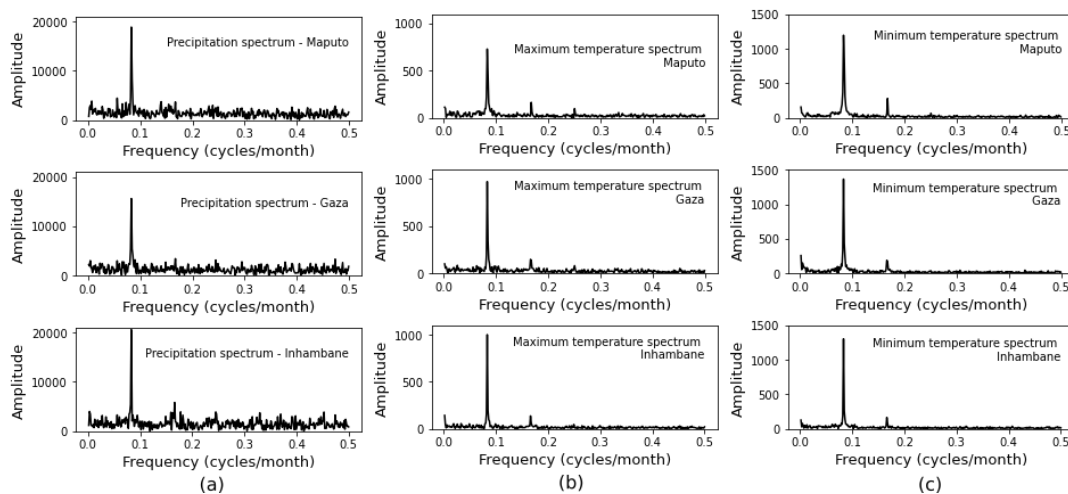


**Figure 4** - Fourier spectrum of (a) precipitation, (b) maximum temperature and (c) minimum temperature, in the three provinces of the southern region of Mozambique: Maputo (upper panels), Gaza (intermediate panels) and Inhambane (lower panels). The most significant periodicity corresponds to the annual variability at the frequency of approximately 0.083 cycles per month. The data is related to 1960 – 2018.

## Long term variability and trend

Within the variability patterns of the beginning and end dates of the rainy season (Figure 3), a certain predominance of seasons with a late start and an early end in the latest years can be observed, although not very significant. For this reason, the duration of the rainy season showed a slight downward trend over the evaluated period, and this fact is illustrated in Figure 5(b). The calculation of trend by linear regression showed a drop of around 20 days for the rainy season length, during the period of 1960 - 2018, from an average of 195 days to an average of 175 days.

Precipitation is by nature a variable with considerable variability, both spatial and temporal. The total precipitation during the rainy season fluctuates around an average of 710 mm, without a clear trend. Overall, the rainy season showed a slight tendency to a decrease of rainfall in the provinces of Gaza and Inhambane, while in Maputo a slight increase is noticeable, as can be seen in Figure 5(a) and in the Table 2 where a comparison between the averages of precipitation during the first and the last 30 years of the studied period is made. The average of precipitation intensity during the rainy season showed a tendency to an

increase, and it is more evident in the province of Maputo, as can be seen in Figure 5(c). This scenario demonstrates that the decrease of the duration of the rainy season along the studied period is significant. In other words, the average intensity of precipitation tends to increase as a result of the decrease in the duration of the rainy season with a slope higher than that of total precipitation. Therefore, one hypothesis can be admitted from this result, it is likely that the occurrence of precipitation in the recent years is more associated with the occurrence of extreme events, since it tends to occur with greater intensity in a relatively short period.

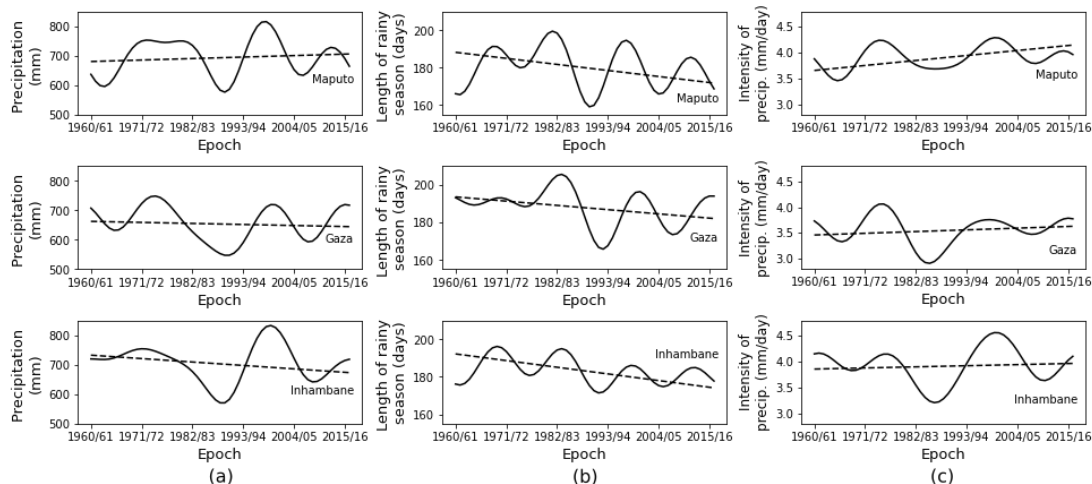


**Figure 5** – Rainy season behavior in the three provinces of the southern region of Mozambique: Maputo (upper panels), Gaza (intermediate panels) and Inhambane (lower panels). The decadal variability (solid line) and the linear trend (dashed line) of: (a) the total precipitation during the rainy season, (b) the rainy season length, and (c) the average intensity of precipitation. The data is related to 1960-2018.

This trend in precipitation converges to the IPCC-AR5 projections for Austral Africa in the summer months (DJF), as can be observed in Figure 7 (Hartmann et al., 2013). The projections pointed to a slight decrease in precipitation of about -10% in the northern region and a slight increase of the same order in the southern region of Mozambique during the period of 2016 - 2035, based on the intermediate scenario of greenhouse gas emission policy designated by the acronym RCP4.5.

On the other hand, the maximum and minimum temperatures showed a clear upward trend. This observation is valid for the three provinces of the southern Mozambique, as can be seen in Figure 6. The linear trend showed that during the period under analysis, the maximum temperature increased by about 0.65 °C within the uncertainty range of 0.5 to 0.8 °C, that is, analyzing the three provinces separately in the region there is a minimum increase of 0.5 °C in the province of Gaza and a maximum of 0.8 °C in the province of Maputo. The minimum temperature increased by about 1.2 °C within the uncertainty range of 0.5 to 1.9 °C. In addition, a comparison between the averages of the first and the last 30 years of the studied period (Table 2) shows an average increase of 0.4 °C in the maximum temperature and an average increase of 0.7 °C in the minimum temperature. Therefore, the minimum temperature has been increasing with a slightly higher rate than the maximum temperature. This implies

that the diurnal temperature range has been decreasing along the last decades. Christy et al. (2009) also verified this scenario for the eastern part of Africa.

The warming rate is of at least  $0.1\text{ }^{\circ}\text{C}$  per decade for the maximum temperature and of at least  $0.15\text{ }^{\circ}\text{C}$  per decade for the minimum temperature. An important aspect to focus attention on is the fact that a greater slope of warming was observed during the period between the 70s and 90s decades, for approximately 20 years. The mean air temperature increased significantly during this period, and from the 90s on, the warming continues but at a reduced rate, as if it tends to stabilize remaining high and approximately stable over the last decades.

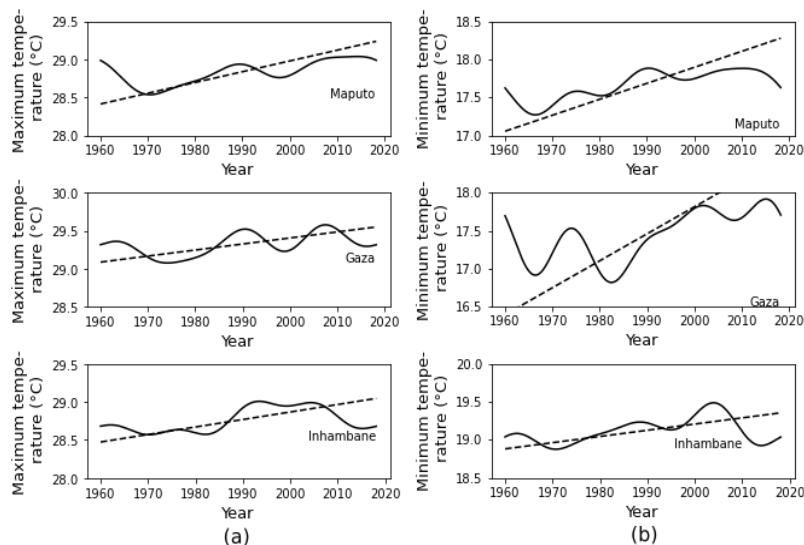


**Figure 6** - Decadal variability (solid line) and the linear trend (dashed line) of (a) maximum temperature and (b) minimum temperature in the three provinces of the southern region of Mozambique: Maputo (upper panels), Gaza (intermediate panels) and Inhambane (lower panels). The data is related to the period of 1960-2018.

It is important to note that this temperature behavior also converges to the observations and projections reported by the IPCC-AR5 regarding the temperature anomalies over the Austral Africa. It is illustrated in Figure 8. There was an increase in temperature of about  $0.8\text{ }^{\circ}\text{C}$  in observations from 1901 to 2012 (see Figure 8a), and it is still expected to continue increasing by about  $0.8\text{ }^{\circ}\text{C}$  in the projections for the period of 2016 – 2035 (see Figure 8b) based on the RCP4.5 scenario (Hartmann et al., 2013).

**Table 2 - Climate averages of precipitation and extreme temperatures for the first and the last 30 years of the period of 1960 - 2018 in the southern region of Mozambique.**

Annual precipitation (mm)			
Province	First 30 years (1960 - 1989)	Last 30 years (1988 - 2017)	All period
Maputo	791	794	794
Gaza	794	765	786
Inhambane	831	827	836
Annual average of maximum temperature (°C)			
Province	First 30 years (1960 - 1989)	Last 30 years (1988 - 2017)	All period
Maputo	28.6	29.0	28.8
Gaza	29.2	29.5	29.3
Inhambane	28.5	29.0	28.8
Annual average of minimum temperature (°C)			
Province	First 30 years (1960 - 1989)	Last 30 years (1988 - 2017)	All period
Maputo	17.4	18.0	17.7
Gaza	16.8	18.0	17.4
Inhambane	19.0	19.3	19.1

## Persistence

The *R/S* analysis was applied to determine the persistence of the climate series and the Hurst exponent varied from 0.51 to 0.85. This range indicates that the series were persistent, what means that the correlation between past and future trends exists and is positive. On the other hand, the possibility of random occurrence of the evaluated series is minimal. The behavior observed in the climate series is more likely to persist for a long period in the future.

According to Mandelbrot and Wallis (1969), when  $0 < H < 1$  the occurrence of the phenomenon presents self-similarities as those of the fractal. Therefore, here another important parameter for the characterization of atmospheric phenomena is determined, the fractal dimension *D* that ranged from 1.15 to 1.49. A change of scale in the sampling of the series would lead to approximately the same result. Table 3 shows the Hurst exponent and the fractal dimension for precipitation, maximum and minimum temperatures, duration of the rainy season and the average intensity of precipitation during the rainy season in the three provinces of the southern region of Mozambique.

**Table 3 – The Hurst exponent *H* and the fractal dimension *D* for all evaluated time series.**

Variable	Maputo		Gaza		Inhambane	
	<i>H</i>	<i>D</i>	<i>H</i>	<i>D</i>	<i>H</i>	<i>D</i>
Precipitation	0.53 ± 0.006	1.47	0.65 ± 0.026	1.35	0.61 ± 0.015	1.39
Maximum temperature	0.67 ± 0.014	1.33	0.62 ± 0.010	1.38	0.83 ± 0.046	1.17
Minimum temperature	0.67 ± 0.036	1.33	0.85 ± 0.041	1.15	0.67 ± 0.027	1.33
Rainy season length	0.64 ± 0.022	1.36	0.67 ± 0.009	1.33	0.57 ± 0.011	1.43
Intensity of precipitation during the rainy season	0.51 ± 0.017	1.49	0.77 ± 0.010	1.23	0.81 ± 0.010	1.19



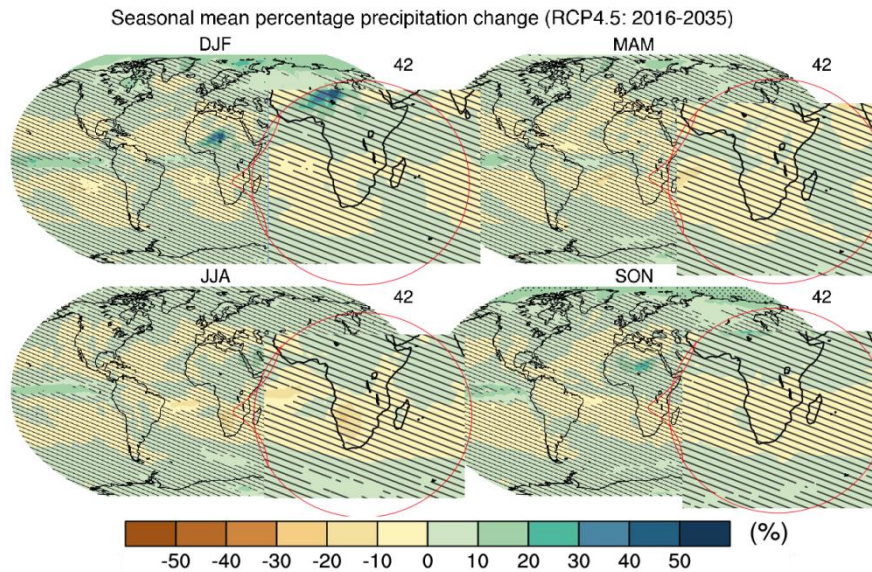


**Figure 7** - CMIP5 multi-model ensemble mean of projected changes (%) in precipitation for 2016 – 2035 relative to 1986 – 2005 under RCP4.5 scenario, for the four seasons. The number of CMIP5 models used is indicated in the upper right corner. Central and Southern Africa is surrounded in red. On average the diagrams indicate negative anomalies (-10%) in Mozambique, however a positive anomaly is also expected for summer months (DJF) in the southern Mozambique. The seasons are indicated at the top of each diagram (Source: Hartmann et al., 2013).

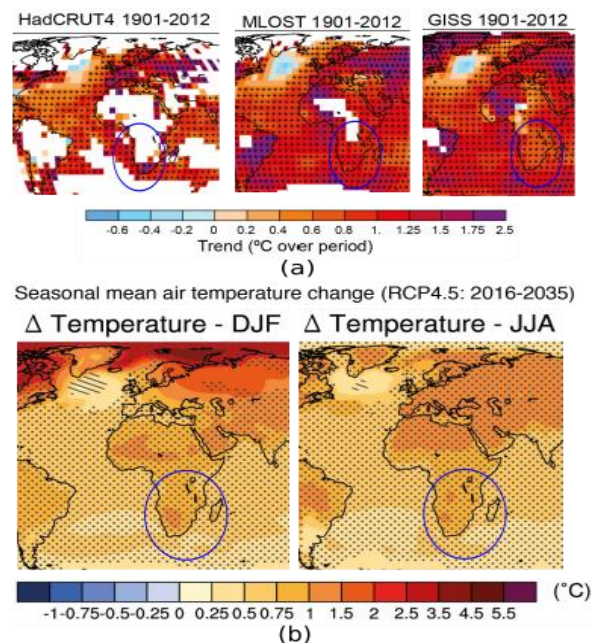


**Figure 8** - Global trends in surface air temperature: (a) observed anomalies analyzing three databases (HadCRUT4, MLOST and GISS) from 1901 to 2012, where the white areas indicate incomplete or missing data; (b) CMIP5 multi-model ensemble mean of projected changes in summer (DJF) and winter (JJA) seasons for the period of 2016 – 2035 relative to 1986 – 2005 under RCP4.5 scenario. In all images the areas surrounded in blue include the southern region of Mozambique (Source: Hartmann et al., 2013).

## CONCLUSIONS

Overall, the obtained results are in line with the observations and projections reported by the IPCC-AR5 regarding the Austral Africa, which includes Mozambique. In the southern region of Mozambique the rainy season extends from the first week of October to the last week of April. The total precipitation during the rainy season fluctuates around an average of 710 mm, presenting unclear trend. The duration of rainy season has shown a decrease and on average it has dropped about 20 days during the period of 1960 - 2018. Analysis in the three provinces separately have shown that the province of Gaza presents the lowest rainfall of the southern region of Mozambique. Although there was some frequency of dry events during the rainy season, in general the rainfall regime throughout the region is still favorable for the development of the main crops practiced under dry land conditions (such as maize, cassava, peanuts, etc.), as long as these events do not occur in the phases of greatest water need of the plant. On the other hand, there was a clear indication of warming, that is, an increase in temperature over the studied period. The maximum temperature increased by about 0.65 °C and the minimum temperature increased by about 1.2 °C during the period of 1960 - 2018. The warming rate is of at least 0.1 °C per decade for maximum temperature and of at least 0.15 °C per decade for minimum temperature, implying that the diurnal temperature range has been decreasing due to the rapid increase in minimum temperature compared to the maximum. All climate series showed persistency with the Hurst exponent ranging from 0.51 to 0.85. In this way, the probability of a random behavior in the climate variables is minimal, and it is more likely that the observed trends prevail for a long period in the future. Besides, the fractal dimension values ranging from 1.15 to 1.41 indicate that the climate series present some self-similarities so that a certain change in the sampling scale of the data would lead to approximately the same results.

## ACKNOWLEDGMENTS

This work was carried out with the support of the Coordenação de Aperfeiçoamento de Pessoal de Nível Superior - Brasil (CAPES) – Financing Code 001. Jone Medja thanks the Universidade Eduardo Mondlane (Departamento de Engenharia Rural) and the program GCUB/ProAfri for sponsoring his MSc. studies at UFBA.

## REFERENCES

- Bagnouls, F. and Gaussen, H. (1957). Les climats biologiques et leurs classifications, *Annales de Géographie*, 66:193–220.
- Bracewell, R. (1999). *The Fourier Transform & Its Applications*, 3rd ed., McGraw-Hill, London, 624p.
- Christy, J. R., Norris, W. B. and McNider, R. T. (2009). Surface temperature variations in east Africa and possible causes, *Journal of Climate*, 22:3342–3356.
- Feder, J. (1989). *Fractals*. 1<sup>st</sup> edition. Plenum Press, New York. 265p.
- Hartmann, D. L., Klein Tank, A. M. G., Rusticucci, M., Alexander, L. V., Brönnimann, S., Charabi, Y. A. R., Dentener, F. J., Dlugokencky, E. J., Easterling, D. R., Kaplan, A., Soden, B.

- J., Thorne, P. W., Wild, M., & Zhai, P. (2013). Observations: Atmosphere and surface. In *Climate Change 2013 the Physical Science Basis: Working Group I Contribution to the Fifth Assessment Report of the Intergovernmental Panel on Climate Change* (Vol. 9781107057999, pp. 159–254). Cambridge University Press.
- Hurst, H. (1951). Long term storage capacity of reservoirs. *Transactions of the American Society of Civil Engineers*, 116:770–799.
- Machado, M. A. M., Sedyama, G. C., Costa, J. M. N., Costa, M. H. (1996). Duração da estação chuvosa em função das datas de início do período chuvoso para o estado de Minas Gerais, *Revista Brasileira de Agrometeorologia*, Santa Maria, 04:73–79.
- Marengo, J. A., Liebmann, B., Kousky, V. E., Filizola, N. P., and Wainer, I. C. (2001). Onset and end of the rainy season in the Brazilian Amazon Basin, *Journal of Climate*, 14:833–852.
- Mandelbrot, B. (1967). How Long Is the Coast of Britain? Statistical Self-Similarity and Fractional Dimension. *Science*, 156(3775), 636–638.
- Mandelbrot, B. and Wallis, J. (1969). Computer experiments with fractional Gaussian noises. Parts 1,2,3. *Water Resources Research*, 5(1):228–267.
- Sansigolo, A. (1989). Variabilidade interanual da estação chuvosa em São Paulo: Climanálise, 04: 40–43.
- Smithson, P. A. (2002). *Climate change 2001, the scientific basis, Contribution of Working Group I to the Third Assessment Report of the Intergovernmental Panel on Climate Change*, edited by J. T. Houghton, Y. Ding, D. J. Griggs, M. Noguer, P. J. Van der Linden, X. Dai, K. Maskell and C. A. Johnson, Cambridge University Press, 881p.